Materials & Design 205 (2021) 109749

Contents lists available at ScienceDirect

Materials & Design

journal homepage: www.elsevier.com/locate/matdes

Modification of heat-induced whey protein isolate hydrogel with highly bioactive glass particles results in promising biomaterial for bone tissue engineering

Michal Dziadek [a,b,c,*], Katarzyna Charuza [d], Radmila Kudlackova [e,f], Jenny Aveyard [g], Raechelle D'Sa [g], Andrada Serafim [h], Izabela-Cristina Stancu [h], Horia Iovu [h,i], Jemma G. Kerns [j], Sarah Allinson [k], Kinga Dziadek [l], Piotr Szatkowski [d], Katarzyna Cholewa-Kowalska [b], Lucie Bacakova [e], Elzbieta Pamula [d], Timothy E.L. Douglas [c,m]

[a] Faculty of Chemistry, Jagiellonian University, Krakow, Poland
[b] Department of Glass Technology and Amorphous Coatings, AGH University of Science and Technology, Krakow, Poland
[c] Engineering Department, Lancaster University, Lancaster, United Kingdom
[d] Department of Biomaterials and Composites, AGH University of Science and Technology, Krakow, Poland
[e] Department of Biomaterials and Tissue Engineering, Czech Academy of Sciences, Prague, Czech Republic
[f] Technical University of Liberec, Liberec, Czech Republic
[g] School of Engineering, University of Liverpool, Liverpool, United Kingdom
[h] Advanced Polymer Materials Group, University Politehnica of Bucharest, Bucharest, Romania
[i] Academy of Romanian Scientists, Bucharest, Romania
[j] Lancaster Medical School, Lancaster University, Lancaster, United Kingdom
[k] Biomedical and Life Sciences Department, Lancaster University, Lancaster, United Kingdom
[l] Department of Human Nutrition and Dietetics, University of Agriculture in Krakow, Krakow, Poland
[m] Materials Science Institute (MSI), Lancaster University, Lancaster, United Kingdom

HIGHLIGHTS

- Newly formulated hydrogels made of whey protein isolate and bioactive glass were created.
- Heat-induced gelation technique used allowed generation of ready-to-use, sterile materials.
- Bioactive glass particles were homogenously distributed in the hydrogel matrix.
- Hydrogels showed a high capacity for mineralization and antioxidant activity.
- Materials were cytocompatible and supported MG-63 osteoblastic cell functions.

GRAPHICAL ABSTRACT

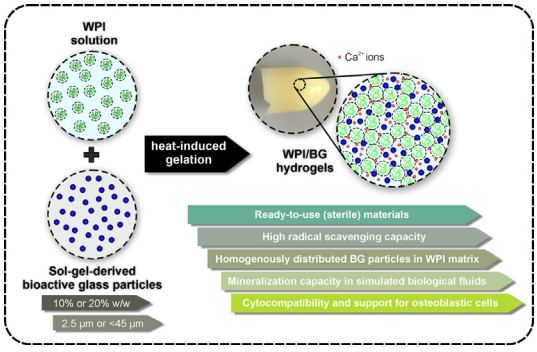

ARTICLE INFO

Article history:
Received 24 January 2021
Revised 14 April 2021
Accepted 15 April 2021
Available online 20 April 2021

ABSTRACT

This study deals with the design and comprehensive evaluation of novel hydrogels based on whey protein isolate (WPI) for tissue regeneration. So far, WPI has been considered mainly as a food industry by-product and there are very few reports on the application of WPI in tissue engineering (TE). In this work, WPI-based hydrogels were modified with bioactive glass (BG), which is commonly used as a bone substitute material. Ready-to-use, sterile hydrogels were produced by a simple technique, namely heat-induced gelation. Two different concentrations (10 and 20% w/w) of sol–gel-derived BG particles of

* Corresponding author at: Faculty of Chemistry, Jagiellonian University, Krakow, Poland.
E-mail addresses: michal.dziadek@uj.edu.pl, dziadek@agh.edu.pl (M. Dziadek).

https://doi.org/10.1016/j.matdes.2021.109749
0264-1275/© 2021 The Author(s). Published by Elsevier Ltd.
This is an open access article under the CC BY license (http://creativecommons.org/licenses/by/4.0/).

Keywords:
Waste material
Mineralization
Enzymatic degradation
Antioxidant activity
Dynamic mechanical analysis
Micro-computed tomography

two different sizes (2.5 and <45 μm) were compared. μCT analysis showed that hydrogels were highly porous with almost 100% pore interconnectivity. BG particles were generally homogenously distributed in the hydrogel matrix, affecting pore size, and reducing material porosity. Thermal analysis showed that the presence of BG particles in WPI matrix reduced water content in hydrogels and improved their thermal stability. BG particles decreased enzymatic degradation of the materials. The materials underwent mineralization in simulated biological fluids (PBS and SBF) and possessed high radical scavenging capacity. *In vitro* tests indicated that hydrogels were cytocompatible and supported MG-63 osteoblastic cell functions.

© 2021 The Author(s). Published by Elsevier Ltd. This is an open access article under the CC BY license (http://creativecommons.org/licenses/by/4.0/).

1. Introduction

Bone tissue is a natural composite with a complex, architectural structure and unique properties, which makes the design of a suitable replacement very demanding [1]. Therefore, tissue engineering (TE) has become a popular approach in the treatment of damaged bone tissue in recent years. Various types of biomaterials have been used for bone regeneration [2]. Much attention has been paid to hydrogels – three-dimensional cross-linked polymer networks which retain a large amount of water. Hydrogels have many advantages; they demonstrate comparable mechanical properties to soft tissues, and it is relatively easy to modify them and adjust their properties. However, the major disadvantages of these materials, from the point of view of bone tissue regeneration, are low mechanical strength and lack of bioactivity, i.e. the formation of a direct chemical bond with bone and promotion of the regeneration processes. Therefore, attempts to combine hydrogels with other components to improve these features and mimic the structure of natural bone tissue have been undertaken [3].

An interesting substance that is able to form a hydrogel is whey protein isolate (WPI). WPI consists of many proteins, mainly β-lactoglobulin, with smaller amounts of α-lactalbumin, serum albumin and other milk proteins. Cross-linking of β-lactoglobulin is most commonly achieved by thermal treatment. The temperature-induced gelation results from peptide denaturation and aggregation processes via covalent intermolecular bonds (thiol (–SH)/disulfide (S–S) interchange reactions) and other intermolecular non-covalent interactions (van der Waals, electrostatic and hydrophobic interactions) [4]. Two indisputable practical advantages of WPI are low cost and availability in vast amounts due to the large size of the dairy industry worldwide. So far, WPI has been considered mainly as a food waste and there are very few reports on the application of WPI in TE. Recently, it has been shown that WPI added to cell culture medium promotes bone cell proliferation and osteogenic differentiation *in vitro* [5,6]. Our recent studies clearly indicated that WPI is also a promising biomaterial for TE in the form of composite hydrogels. It was shown that enzymatic mineralization of WPI hydrogels [7] as well as the incorporation of a ceramic phase, such as calcium phosphate [8] and aragonite [9] in WPI-based matrices significantly altered the properties relevant for bone regeneration applications (swelling and degradation rate, mechanical performance, microstructural features, osteoblastic cell response).

Incorporating a bioactive inorganic phase in the hydrogel matrix will also assure direct chemical bonding with bone and lead to improved roughness and local stiffness which will enhance the attachment, proliferation and differentiation of osteoblasts and further increase the integration of the material in the surrounding bone tissue [10]. Particularly innovative in those processes is the use of bioactive glasses (BGs). The products of BG dissolution assure osteoinductivity, as silica and calcium ions stimulate osteogenic genes' expression, further modulation of osteogenesis and bone formation [11]. Furthermore, sol–gel-derived BGs, because of their high surface area and the presence of silanol groups (Si-OH) in their structure, show enhanced chemical reactivity in biological environments in comparison with conventional melt-derived glasses [12]. Our previous studies indicated that fast and massive Ca^{2+} ion release from sol-gel-derived, calcium-rich BGs accelerates rapid nucleation and crystallization of calcium phosphate layers [13] and also alters the properties of hydrogel-based materials, e.g. gelation process, antibacterial activity [14,15].

Building on the promising results of our previous studies, in this work hydrogel biomaterials made of WPI were modified by incorporation of gel-derived calcium-rich BG particles. The study involved investigation of the effect of (a) different concentrations of BG particles in WPI matrix as well as (b) various BG particle sizes on (i) distribution of BG particles in the hydrogel matrix, as well as its microstructure and porosity; (ii) thermal stability and thermal degradation processes; (iii) compressive strength; (iv) viscoelastic properties; (v) swelling behaviour and hydrolytic degradation in different media; (vi) enzymatic degradation; (vii) *in vitro* mineralisation process of hydrogels; (viii) radical scavenging capacity; (ix) *in vitro* MG-63 osteoblastic cell response; and (x) antibacterial activity against *S. aureus*. To the best of our knowledge, this is the first such comprehensive and in-depth study on WPI-based composite hydrogels modified with BG particles for potential regeneration of non-load bearing bone tissue defects.

2. Methods

2.1. Preparation of WPI/BG composite hydrogels

BG powder of the following composition (%mol) 54CaO-40SiO_2-6P_2O_5, denoted as A2, was synthetized using a sol–gel technique as reported previously [16]. Two sizes of BG particles were used: 2.5 μm (d_{50}) and < 45 μm.

WPI-based hydrogels with the addition of 10% or 20% w/w of BG particles of 2.5 μm (d50) and < 45 μm sizes were produced (hereafter denoted as WPI/10$A2_{2.5}$, WPI/20$A2_{2.5}$, WPI/10$A2_{45}$, WPI/20$A2_{45}$, respectively). WPI solution (40 w/v%) was prepared by dissolving WPI powder (Davisco, USA) in deionised water (dH_2O) in an ultrasonic bath for 30 min below 35 °C. 0.5 ml of the solution were then mixed with the correct amount of BG powder in 2 ml Eppendorf tubes. Samples were then homogenised using a vortexer for 10 s and preheated at 90 °C during continuous mixing (3000 rpm) with a ThermoMixer C (Eppendorf, Germany) for 3 min to prevent BG sedimentation. Finally, materials were autoclaved for 15 min at 121 °C. WPI hydrogels with no addition of BG particles served as control samples.

2.2. Micro-computed tomography (μCT) analysis

μCT scans were recorded using a SkyScan 1272 high-resolution X-Ray microtomograph (Bruker MicroCT, Belgium). The samples were scanned in sealed 2 ml Eppendorf tubes which were fixed

on the sample holder using modelling clay. All samples were scanned without filter at a voltage of 50 kV and an emission current of 200 μA. The images were registered at a resolution of 2452 × 1640 and a pixel size of 5 μm, with a rotation step of 0.3°and 3 frames averaging. All images were processed using CT NRecon software (Version 1.7.1.6) and reconstructed as 3D objects using CTVox (Version 3.3.or1403). DataViewer was employed for detailed visualization of the transverse and longitudinal cross sections of the samples. Quantitative analysis of the porosity of the tested samples was performed using CT Analyzer software (Version 1.17.7.2). The reconstructed cross-sections obtained following micro-CT scanning were loaded into the software and the sample was divided into three sections, each containing 500 slices.

2.3. Thermogravimetric analysis (TGA)

Thermal stability and thermal degradation processes of hydrogels were determined on the basis of the results of thermogravimetric analysis (TGA) and differential thermogravimetric analysis (DTG). The measurements were performed using a Discovery TGA 550 analyser (TA Instruments, USA) in the temperature range from 35 to 600 °C at a heating rate of 10 °C min^{-1}, under a nitrogen atmosphere. The samples (c.a. 10 mg) were placed in a platinum crucible.

2.4. Compression tests

Mechanical strength of hydrogels was determined using an Inspekt 5 Table Blue testing machine (Hegewald & Peschke, Germany) equipped with a 100 N load cell. Samples were cut into cylinders of 10 mm height and compressed with a displacement rate of 5 mm min^{-1} (n = 10). Then, Young's modulus (E_C) and the stresses corresponding to compression of a sample by 50% ($\sigma_{50\%}$) were measured. The results were expressed as mean ± standard deviation (SD).

2.5. Dynamic mechanical analysis (DMA)

Viscoelastic properties of hydrogels were determined using dynamic mechanical analysis (DMA). The hydrogels were subjected to a cyclic load (compression) with temperature change over time. The measurements were performed using a Discovery DMA 850 analyser (TA Instruments, USA) in the temperature range from −90° C to 110° C at a heating rate of 3 °C min^{-1}. The frequency of the applied load (1 N) was 10 Hz with an amplitude of 35 μm.

2.6. Swelling tests

Swelling behaviour of hydrogels was investigated by incubating the samples (n = 3) in dH_2O and phosphate buffered saline (PBS; Gibco, USA) at 37 °C. The samples were weighed at the beginning of the experiment and again after 1, 3 and 7 days of incubation. Before weighing the samples were placed on filter paper to remove excess water from the surface. Swelling of each sample was calculated as follows: $\frac{W_t - W_0}{W_0} \times 100\%$, where W_t is weight after specific period of incubation, W_0 is weight before incubation. Materials after incubation were freeze-dried for further analyses. The results were expressed as mean ± standard deviation (SD).

2.7. Bicinchoninic acid (BCA) assay

To assess the level of hydrolytic degradation of hydrogels and protein release to incubation medium, BCA assay was performed using Bicinchoninic Acid Kit (Sigma-Aldrich, USA) according to the manufacturer's protocol after 1, 3, and 7 days of incubation in dH_2O and PBS. The absorbance of samples was measured at 562 nm with a Tecan Infinite M200 PRO plate reader (Tecan Group Ltd., Switzerland). The amount of protein released to the medium was calculated on the basis of a standard curve. The results were expressed as mean ± standard deviation (SD).

2.8. Enzymatic degradation

Enzymatic degradation of hydrogels was investigated by incubating the samples (n = 3) in PBS (Gibco, USA) containing 0.025% trypsin (Gibco, USA) and 0.025% subtilisin (Sigma-Aldrich, USA) at 37 °C. The samples were freeze-dried and weighed at the beginning of the experiment and again after 1, 3 and 7 days of incubation. Mass loss of each sample was calculated as follows: $\frac{W_0 - W_t}{W_0} \times 100\%$, where W_0 is the weight of the freeze-dried sample before incubation and W_t is the weight of the freeze-dried sample after a specific period of incubation. The results were expressed as mean ± standard deviation (SD).

2.9. Mineralisation in simulated body fluid (SBF)

The mineralization process of hydrogels was performed by incubation in SBF, prepared according to Kokubo and Takadama [17]. Samples were incubated in SBF for 7 and 14 days at 37 °C in sterile polypropylene containers and then freeze-dried for further analysis. The ratio of the composite hydrogel's weight (g) to the solution's volume (ml) was 1/100.

2.10. Fourier transform infrared spectroscopy (FTIR)

The samples before and after incubation in SBF, PBS, and dH_2O were examined using ATR-FTIR (Cary 630, Agilent Technology, UK) equipped with a diamond crystal. Spectra were collected in the 550–4000 cm^{-1} spectral range with a resolution of 4 cm^{-1} and by averaging 64 scans.

2.11. Scanning electron microscopy (SEM)

SEM analysis was performed before and after incubation of the samples in PBS and SBF. Samples were coated with a carbon layer. SEM analysis was performed using a secondary electron detector JSM-7800F (Jeol UK Ltd., UK). Images were acquired with an accelerating voltage of 5 kV.

2.12. Inductively-coupled plasma optical emission spectrometry (ICP-OES)

The concentrations of calcium and phosphorus in PBS and SBF during incubation of the materials were determined by ICP-OES using a 5100 Synchronous Vertical Dual View Spectrometer (Agilent Technologies, USA). The instrument was calibrated by means of standard solutions. Measurements were taken in triplicate. The results were expressed as mean ± standard deviation (SD).

2.13. Radical scavenging capacity (RSC)

The radical scavenging capacity (RSC) of the hydrogels was evaluated against $ABTS^{\bullet+}$ radical cations (Sigma-Aldrich, USA) according to [18] with some modifications. 10 mg of samples (n = 3) were placed in a test-tube and 3 ml of $ABTS^{\bullet+}$ solution was added, followed by shaking in the dark at 30 °C. The decrease in absorbance at 734 nm was evaluated after 5, 10, and 20 min using a spectrometer (UV-1800, RayLeigh, China). The RSC of the materials was calculated according to the following equation: $RSC = \frac{A_0 - A_t}{A_0} \times 100\%$, where A_0 was the absorbance of $ABTS^{\bullet+}$ solu-

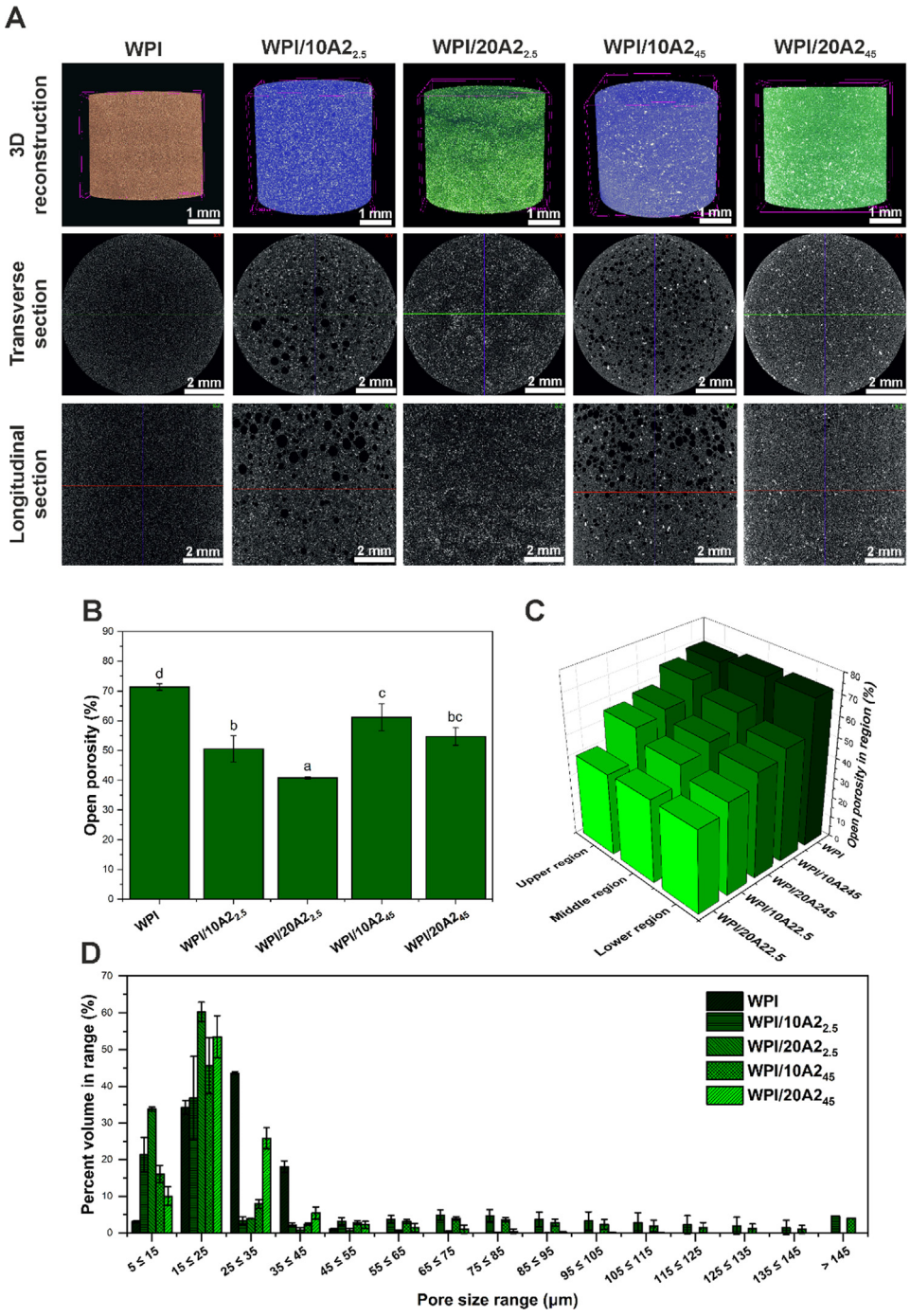

Fig. 1. Representative μCT analyses of the WPI and WPI/BG hydrogels – 3D reconstruction and cross sections (A). White regions – BG particles, dark regions – pores. Quantitative data based on μCT analyses of the WPI and WPI/BG hydrogels: open porosity (B), open porosity distribution (C), and pore size distribution (D). Statistically significant differences ($p < 0.05$) between materials are indicated by subsequent lower Latin letters.

tion before the addition of materials, and A_t was the absorbance of the solution with the sample after a given period of time. The results were expressed as mean ± standard deviation (SD).

2.14. In vitro biological tests

Preliminary *in vitro* cell tests were conducted with osteosarcoma MG-63 cell line (Sigma Aldrich, USA). 9.5×10^3 cells/cm^2 were seeded on 1 mm thick samples in 48-well plate in 1 ml of DMEM culture media (Sigma Aldrich) supplemented with 10% FBS (Thermofisher), 100 IU ml^{-1} of penicillin and 0.1 mg ml^{-1} streptomycin (Sigma Aldrich). Cell culture was conducted at 37 °C, 90% humidity and 5% atmospheric pressure of CO_2.

In order to assess the proliferation of the cells, Cell Titer 96® AQueous One Solution Cell Proliferation Assay (MTS, Promega, USA) was conducted on days 3 and 7 after seeding according to the manufacturer's protocol. Absorbance was measured at 490 nm with Tecan Infinite M200 PRO plate reader (Tecan Group LTD., Switzerland). For all sample groups, n = 3. The results were expressed as mean ± standard deviation (SD).

Adhesion and morphology of cells was observed by fluorescence microscopy 3 and 7 days after seeding. Samples were washed with PBS, fixed with ice cold 70% ethanol for 10 min, then washed with

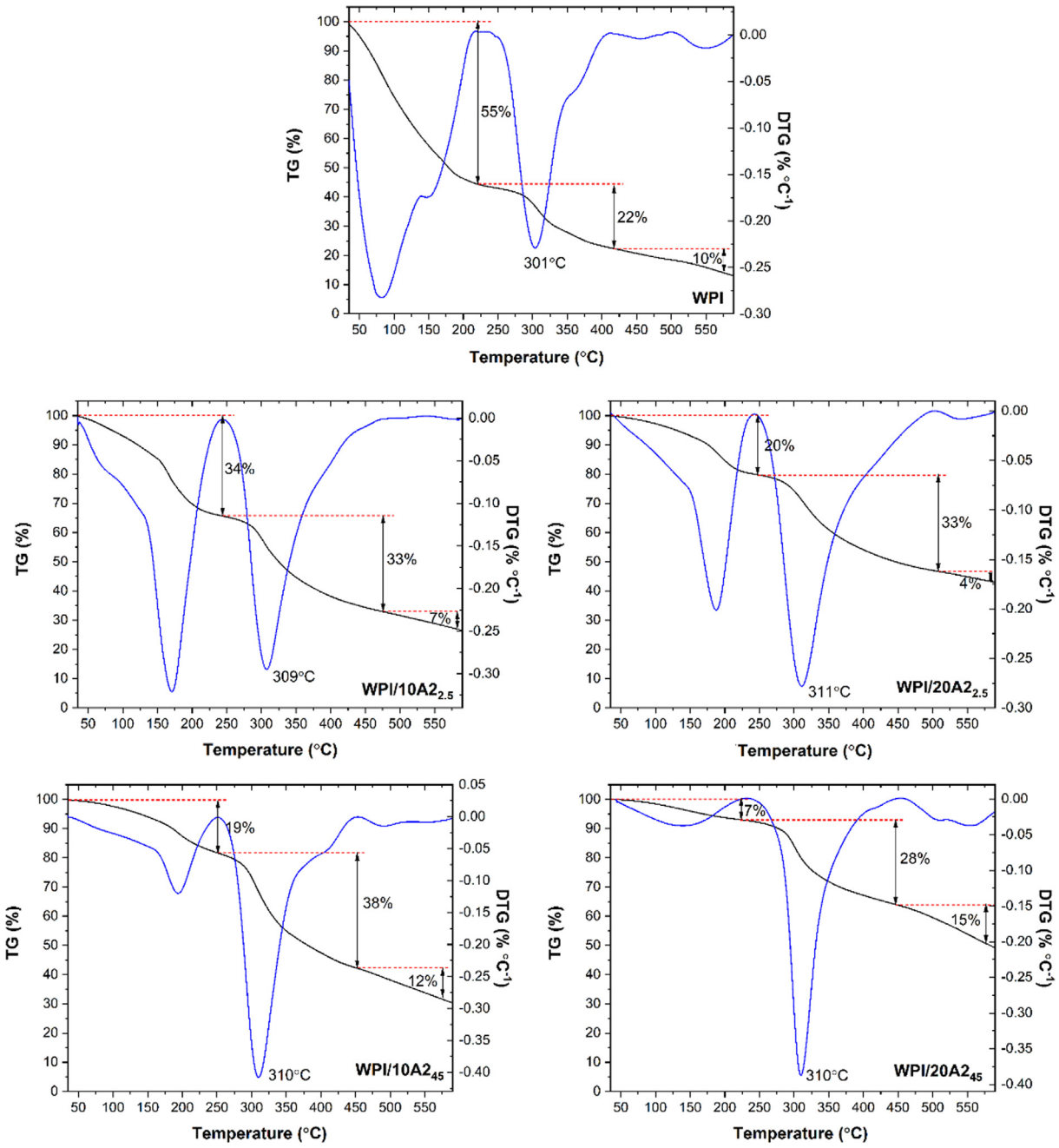

Fig. 2. Thermogravimetric (TG) and derivative thermogravimetric (DTG) curves of the WPI and WPI/BG hydrogels.

PBS and stained with a combination of Texas Red C2-maleimide (cell membrane and cytoplasm; red colour; Invitrogen) and Hoechst #33342 trihydrochloride (nuclei, blue colour; Sigma Aldrich, USA), with final concentrations in PBS equal to 50 ng ml^{-1} and 0.5 μg ml^{-1}, respectively. Staining was conducted at room temperature in the dark for 15 min. After staining, the samples were washed twice with PBS and visualised using an Axio Scope.A1 microscope (Zeiss, Germany).

2.15. Antibacterial activity

The antimicrobial efficacy of hydrogels was determined by colony forming unit (CFU) assays against *S. aureus* bacteria. To determine the time period for antimicrobial activity, bacteria were sampled at 1, 4 and 24 h time points. The CFU assay enumerated the surviving bacterial cells following incubation with a sample. Bacterial cells were incubated with the hydrogel and after 1, 4 and 24 h of contact time, an aliquot of solution was removed, serially diluted and plated on agar to determine the number of bacterial cells remaining in the solution. An overnight culture of *S. aureus* in Luria broth (LB) was diluted to contain 1 × 10^6 CFU ml^{-1} (in LB) and 1 ml was applied to each sample. Samples were then incubated in a shaking incubator at 37 ℃ for the allotted time. After 1, 4 or 24 h, serial dilutions of the bacterial solution were prepared in LB (up to 10^{-10}), and 10 μl of each dilution was plated in triplicate on LB agar using the Miles and Misra method. Following overnight incubation at 37C, colonies were counted. For all sample groups, n = 3. The results were expressed as mean ± standard deviation (SD).

2.16. Statistical analysis

The results were analysed using one-way analysis of variance (ANOVA) with Duncan post-hoc tests, which was performed with Statistica 13.1 software (Dell Inc., USA). The results were considered statistically significant when $p < 0.05$.

3. Results and discussion

3.1. Microstructure evaluation using μCT

The quantitative analysis of μCT results showed that the closed porosity of all hydrogels was below 0.05%; therefore nearly 100% interconnectivity of the pores was obtained. WPI hydrogel revealed a high porosity above 70% (Fig. 1**B**). The presence of BG particles in WPI matrix significantly reduced porosity, which is in agreement with the literature for other hydrogels modified with inorganic fillers [19]. Specifically, the reduction was higher for smaller BG particles and higher concentration of modifiers. Moreover, a heterogeneous distribution of the overall porosity was noticed in the composite materials, with higher values of the open porosity in the upper region of the samples (Fig. 1**C**), as was also observed in μCT longitudinal cross sections (Fig. 1**A**). Similar findings were reported in our previous work on WPI/gelatin/calcium phosphate composites [8]. The analysis of pore size distribution demonstrated that WPI hydrogel had pores predominantly in the range of 25–35 μm, while the pores of the composite samples were mostly in the range of 15–25 μm. Additionally, hydrogels containing 10% of BG exhibited much larger pores. The largest pores were up to 500 μm in diameter. μCT analysis showed that BG particles were generally homogenously distributed in the hydrogel matrix, however, in the case of composite containing 20% of BG, the smaller particles tended to agglomerate, while the bigger ones were concentrated near the edges and bottom of the sample (Fig. 1**A**).

In our recent works, introduction of ceramic particles, namely calcium phosphate [8] and aragonite [9] in WPI-based matrices also resulted in porous materials with much bigger pores compared to unmodified samples. What is more, in contrast to this study, both composites showed inhomogeneous distribution of the fillers in polymer matrices, even though all materials were obtained following the same protocol. This suggests that distribution of fillers in WPI-based matrix depends on their properties (i.e. chemical composition, shape, size, zeta potential, and surface area).

3.2. Thermal and mechanical analysis

The thermogravimetric (TG) and derivative thermogravimetric (DTG) curves of hydrogels are shown in Fig. 2**.** Three noticeable stages of thermal degradation of hydrogels were observed in the temperature range of 35–600 °C. The first degradation stage occurred at approximately 35–250 °C, corresponding to the loss of free, bonded, and interstitial water. The second stage, from approximately 250 to 500 °C is associated with the chemical decomposition of WPI. The third stage took place above 500 °C, corresponding to oxidative degradation of carbon residues formed during the previous stage. In a nitrogen atmosphere, the carbonaceous material formed in the third stage did not undergo complete decomposition [20]. Furthermore, it should be taken into account that WPI contains up to 5% ash.

It was observed that the presence of BG particles in WPI matrix, especially bigger particles and at higher particle concentration, significantly reduced mass loss in the first stage. In addition, the first peak in the DTG curves noticeably shifted to the higher tempera-

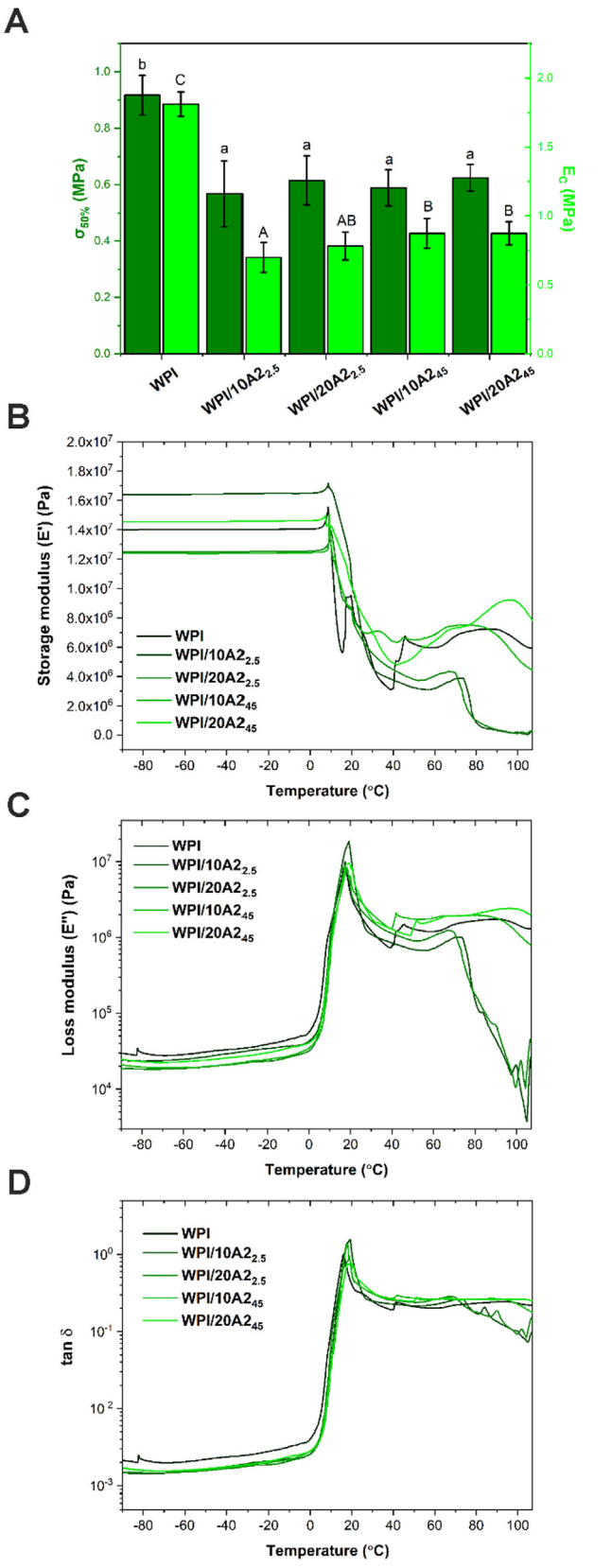

Fig. 3. Compression test results: Stresses corresponding to compression of a sample by 50% and Young's modulus of WPI and WPI/BG hydrogels (A). Statistically significant differences ($p < 0.05$) between materials are indicated by subsequent lower (for $\sigma_{50\%}$) and upper (for E_C) Latin letters. DMA results: storage modulus E' (B), loss modulus E'' (C) and loss factor tan δ (D) curves of the WPI and WPI/BG hydrogels.

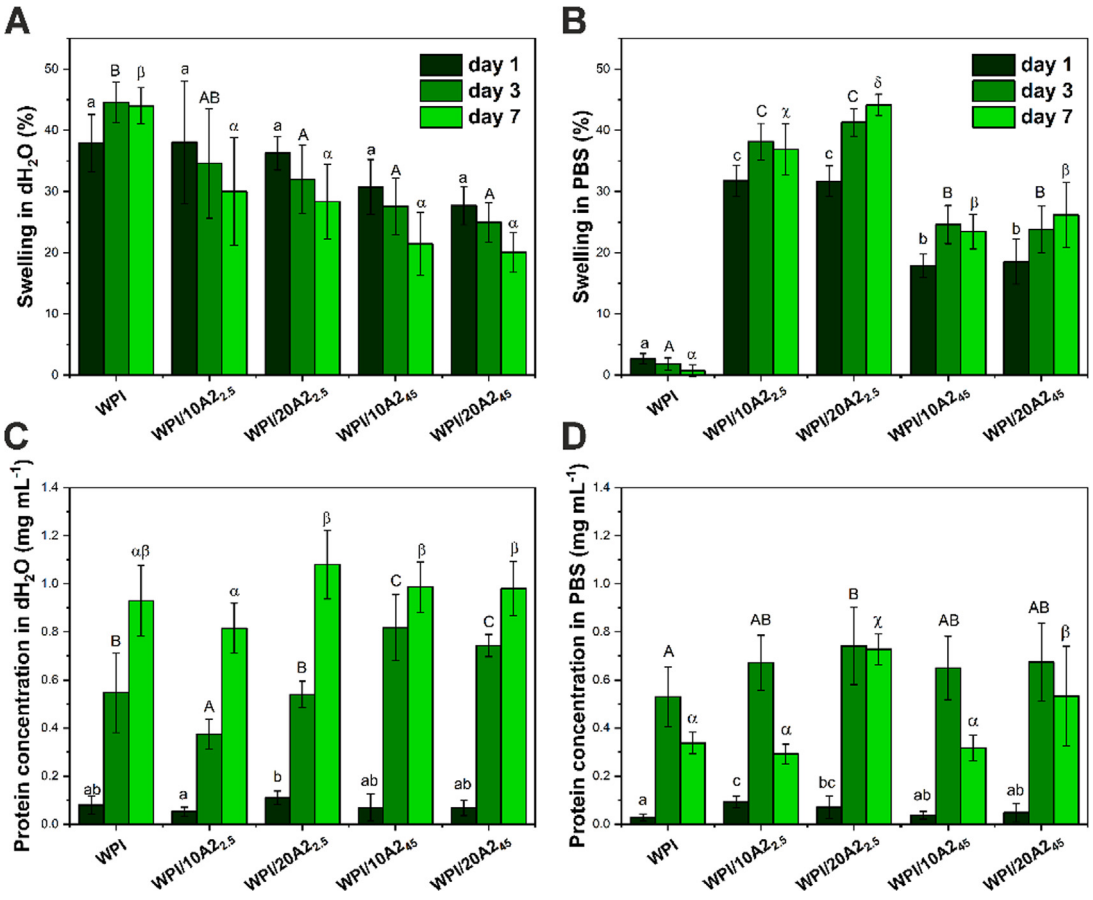

Fig. 4. Swelling of WPI and WPI/BG hydrogels (A, B) and release of proteins (C, D) after incubation in dH_2O (A, C) and PBS (B, D). Statistically significant differences ($p < 0.05$) between materials are indicated by subsequent lower (for 1-day incubation), upper (for 3-day incubation) Latin letters and Greek letters (for 7-day incubation).

tures for composite hydrogels. These results indicated that the presence of BG particles in WPI matrix reduced water content in hydrogels. In the second stage, the degradation temperature of WPI increased upon modification with BG particles from 301 °C for WPI hydrogel to about 310 °C for WPI/BG composite hydrogels. This indicated the improved thermal stability of the composites. Degradation temperature of WPI was in agreement with the literature data obtained for WPI-based materials [21]. Mass loss of composite materials in the second stage was significantly higher compared to WPI hydrogel. This may be related to improved water retention of BG particles in composites. As the sol–gel derived A2 BG exhibits high surface reactivity and high surface area, the formation of additional silanol groups (Si-OH) and increase in content of chemically adsorbed water on BG surfaces may occur under autoclaving conditions during hydrogel preparation. The processes of condensation and elimination of hydroxyl groups as well as volatilization of chemically adsorbed water take place at higher temperatures (above 250 °C) [22].

Mechanical properties of hydrogels were determined using a compression test. As shown in Fig. 3**A**, the incorporation of BG particles led to significant decreases in E_c and $\sigma_{50\%}$. WPI hydrogel exhibited an E_c value of 1.8 MPa. The addition of smaller BG particles (2.5 μm) resulted in values of 0.7 and 0.8 MPa for 10% and 20% of BG, respectively. The presence of both concentrations of 45 μm BG particles resulted in an E_c value of 0.8 MPa. The control sample showed $\sigma_{50\%}$ of 0.9 MPa, while the materials containing BG particles showed similar values of 0.6 MPa.

Deterioration of mechanical properties of the WPI/BG hydrogels may result from the presence of bigger pores, especially for hydrogels with 10% of BG particles (Fig. 1**A and D**), and inhomogeneous

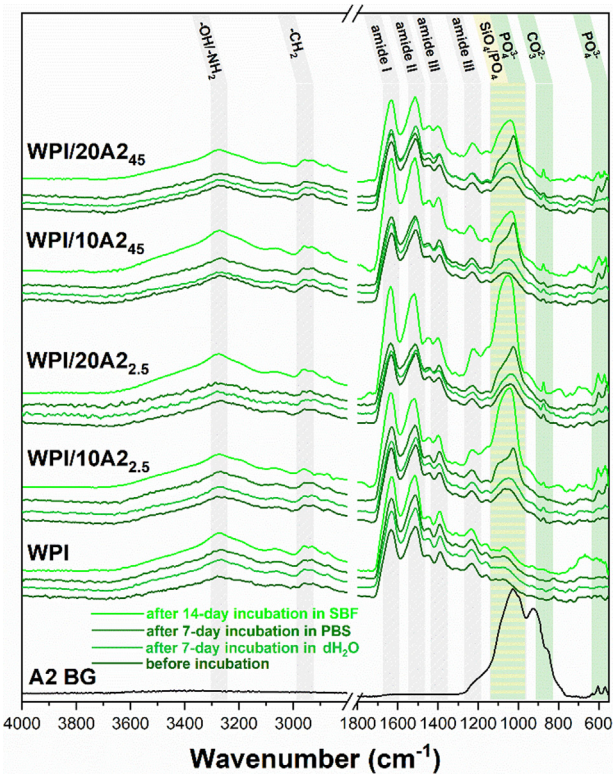

Fig. 5. ATR-FTIR spectra of WPI and WPI/BG hydrogels before and after 7-day incubation in dH_2O and PBS and after 14-day incubation in SBF. For comparison, the FTIR spectrum of A2 bioactive glass is also shown.

distribution of porosity in composite materials (Fig. 1**C**), despite the lower porosity. Although the presence of ceramic fillers in a hydrogel polymer matrix [8,9], and the lower porosity of the material [19] usually results in improved mechanical properties, in this case pore size and distribution seem to be the key factors influencing the strength of materials. Furthermore, in the case of materials with 20% of BG particles, reduced mechanical parameters may be due to the tendency of smaller particles to agglomerate or less homogenous distribution of bigger particles in the WPI matrix. Li et al. [23] showed that a high concentration of TiO_2 reduced Young's modulus and tensile strength of WPI-based films because the polymer network continuity was interrupted by the TiO_2 agglomerates. The hydrogels obtained in this study are only suitable for non-load bearing applications.

Viscoelastic properties of hydrogels were evaluated using dynamic mechanical analysis (DMA). Fig. 3**B-D** show changes in storage modulus (E'), loss modulus(E'') and loss factor tan δ (E''/E') of hydrogels over a temperature range −90–100 °C. All of the materials showed predominantly elastic characteristics, displaying a higher elastic modulus (E') than viscous modulus (E'') over the entire temperature range. In the temperature range −90–10 °C, all hydrogels showed a stiff glassy regions with high values of E' and low values of E'', resulting from the limited mobility of polymer chains additionally trapped between the ice crystals. Above 0 °C, a sudden drop in E' and increase in E'' occurred due to the onset of a thermal transition. Movement of polymer chains and water molecules in hydrogel network was possible, leading to energy dissipation. In the temperature range 30–70 °C, a relatively stable trend in E' and E'' values was observed which is related to the flexible rubbery region. The most significant differences in E' and E'' curves were observed above 70 °C. For WPI/BG composites containing smaller BG particles, a sudden drop in E' and E'' values was observed. This was due to disintegration of the hydrogels. A reason may be that smaller particles caused significant interruption in the polymer network continuity [23], and therefore, after partial water evaporation from hydrogel network, materials lost their mechanical integrity. In the case of WPI as well as WPI/10A2$_{45}$ and WPI/20A2$_{45}$ there was no such distinct changes. Storage modulus of these hydrogels tended to increase, indicating material reinforcement, probably related to partial water evaporation. The strong peak in the tan δ curves revealed the presence of a glass transition temperature (T_g). A shift in T_g to higher values was observed for WPI/BG composites (18 °C ≤ T_g ≤ 20 °C) compared to pure WPI hydrogel (T_g = 16 °C). Furthermore, for composites with 10% of BG particles, increase in peak intensity was observed.

Variations in mechanical properties, water retention capacity and thermal stability between WPI and WPI/BG hydrogels may be attributed to changes in the structure of the WPI-based matrix. On the one hand, divalent cations, such as Ca^{2+} released from BG particles, are able to crosslink negatively charged groups of proteins, enhancing the intermolecular interactions [24]. On the other hand, the presence of Ca^{2+} ions during heat-induced gelation may

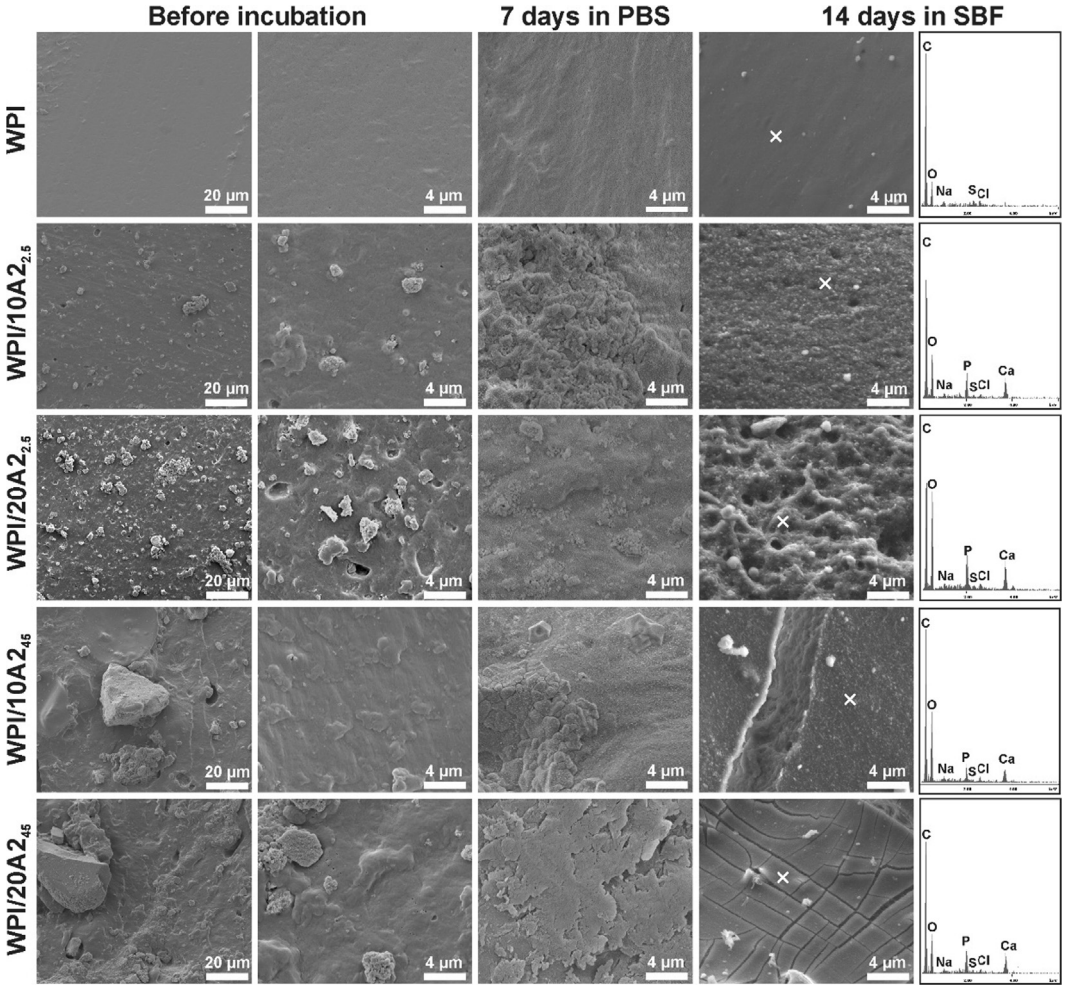

Fig. 6. SEM images of WPI and WPI/BG hydrogels before and after 7-day incubation in PBS and after 14-day incubation in SBF. EDX analyses were performed at the points marked by crosses for the samples incubated in SBF.

result in the formation of weaker, more non-covalent interactions between whey protein chains at the expense of strong, covalent disulfide bonds [25]. Besides the different cross-linking densities and bond strength between the crosslinked protein chains, hydroxyl groups present on the surface of sol–gel-derived BG particles may replace polymer–polymer interactions by developing polymer-BG hydrogen bonding [26]. A shift in T_g on the tan δ curves could confirm changes in intermolecular interaction density [27], as well as enhanced WPI-BG interactions [28].

3.3. Swelling and degradation tests

After incubation in water, in contrast to the control (pure WPI), swelling ability of samples containing BG particles gradually decreased with increasing incubation time, from around 37 to 27% for smaller particles and from 28 to 20% for larger ones (Fig. 4**A**). Incubation in PBS, in contrast to dH_2O, resulted in increased swelling percentage of the WPI/BG hydrogels with increasing incubation time (Fig. 4**B**). Furthermore, it was observed that values noted for WPI/10A2$_{2.5}$ and WPI/20A2$_{2.5}$ materials were in the range 30–45%, materials with 45 μm BG particles between 17 and 25%, while swelling of pure WPI decreased from 3% to 1% at the end of the experiment. The level of swelling both in dH_2O and PBS was higher for samples containing 2.5 μm BG than those with 45 μm particles, which was particularly visible for samples incubated in PBS.

The differences in swelling behaviour between materials incubated in various media, i.e. PBS and dH_2O, were probably caused by differences in the concentration of the ions and pH during thermal gelation and during the swelling process, as well as the buffer capacity of swelling media [29,30]. The ionic groups of the hydrogel are able to immobilise counterions, depending on the conditions, such as pH. Thus, during incubation in the swelling medium an osmotic pressure is generated across the hydrogel, resulting in a water uptake (swelling) or water loss (shrinking). As shown in our previous works, rapid dissolution of A2 BG resulted in alkalisation of aqueous media, depending on medium type (buffer solution/dH_2O) and size of BG particles [14,31]. Smaller size particles and their higher surface area resulted in higher contact area with the solution during hydrogel preparation as well as during swelling tests, resulting in faster release of Ca^{2+} ions and pH changes. Changes in swelling between WPI and WPI/BG hydrogels may also result from additional interfaces between BG particles and polymer matrix working as microvoids that would allow faster diffusion of incubation medium. On the other hand, incubation of the WPI/BG materials in buffer containing phosphate ions (PBS) and massive release of Ca^{2+} ions from BG structure resulted in formation of a new mineral phase – calcium phosphate (Figs. 5 and 6), affecting mass changes measurements. What is more, mass changes were also influenced by WPI matrix degradation, as was observed during protein release measurements (Fig. 4**C-D**).

3.4. Material analysis after incubation in different media

The ATR-FTIR spectra of A2 glass and WPI-based hydrogels incubated in PBS and dH_2O for 7 days and in SBF for 7 and 14 days are presented in Fig. 5. The band around 3270 cm^{-1} corresponds to stretching vibrations of –OH and $–NH_2$ groups. Weak bands observed at 2950 cm^{-1} are connected with stretching vibrations of $–CH_2$ groups. The bands at 1640, 1520, 1385, and 1240 cm^{-1} are characteristic for primary (C = O stretching), secondary (N-H bending coupled with C-N stretching), and tertiary (C-N stretching and N-H bending) amide groups of proteins, respectively [32]. The spectra of the WPI/BG hydrogels contain additional bands due to

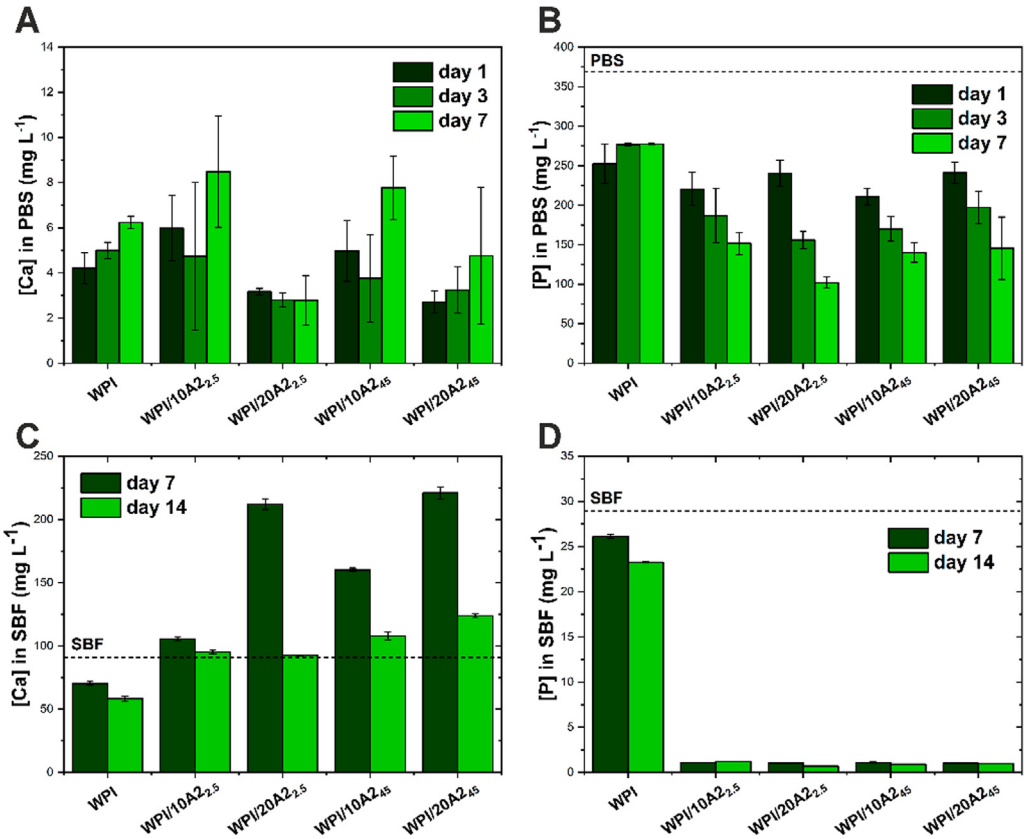

Fig. 7. Concentration of Ca (A,C) and P (B,D) in PBS (A,B) and SBF (C,D) after incubation of WPI and WPI/BG hydrogels.

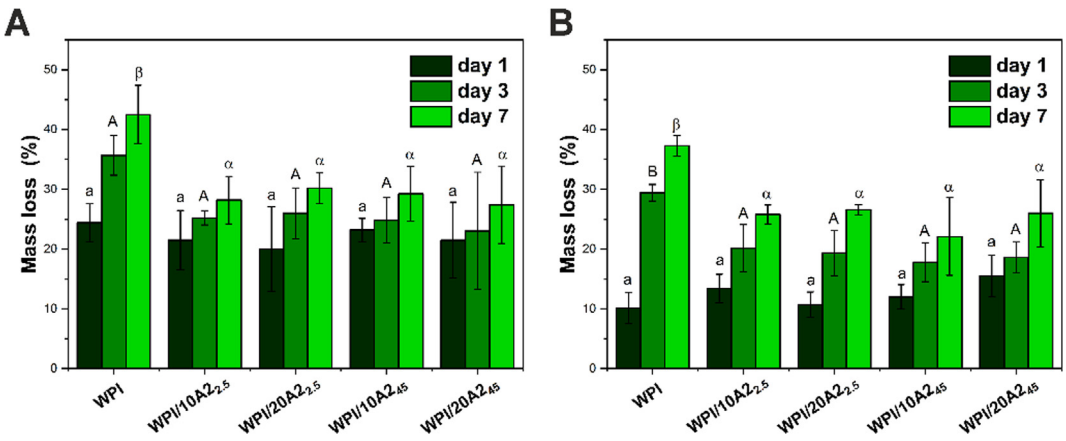

Fig. 8. Mass loss of WPI and WPI/BG hydrogels after incubation in trypsin (A) and subtilisin (B) solutions. Statistically significant differences ($p < 0.05$) between materials are indicated by subsequent lower (for 1-day incubation), upper (for 3-day incubation) Latin letters and Greek letters (for 7-day incubation).

the presence of BG. A broad new band between 1140 and 890 cm^{-1} is assigned to the stretching vibrations of SiO_4 and PO_4 tetrahedra [16].

After incubation in PBS, SBF, and dH_2O, there were no significant changes in the spectra of WPI hydrogel. The spectra of WPI/BG materials after incubation in PBS and SBF contain new bands. A band observed between 960 and 1130 cm^{-1} corresponds to stretching vibrations of PO_4^{3-} groups. A double band in the range of 600–560 cm^{-1} indicates the formation of crystalline calcium phosphate (CaP) and is related to the bending vibrations of PO_4^{3-}-groups [33]. This can confirm mineralisation of WPI/BG hydrogels. The spectra of WPI/BG hydrogels incubated in PBS and SBF display a new band at 874 cm^{-1} which can be assigned to CO_3^{2-} bending vibrations. This may indicate that the CaP phase which crystalizes during incubation was carbonated hydroxyapatite [34]. Furthermore, a new band of low intensity at 800 cm^{-1} appeared in the spectra of composites with smaller BG particles after incubation in SBF, which may be related to silica groups in the CaP/silica gel layer. In the case of composites with smaller BG particles incubated in SBF, the bands characteristic of a CaP phase exhibited higher intensities compared to materials with < 45 μm particles. This may indicate an enhanced mineralization of these composites. A reason may be that smaller particles were more exposed on the surfaces of WPI/BG hydrogels and they have a higher surface area compared to larger ones. This led to faster release of Ca^{2+} ions from the BG structure and faster supersaturation of the incubation medium, accelerating nucleation and crystallization of the CaP phase.

SEM images of WPI-based hydrogels before and after incubation in PBS and SBF are shown in Fig. 6. Analysis of the samples before incubation showed that BG particles of both sizes were homogeneously distributed in WPI hydrogels. Smaller particles formed single, small agglomerates, which were also evenly distributed in the WPI hydrogel matrix.

After incubation in both media, namely PBS and SBF, WPI/BG hydrogels showed morphological changes. As confirmed by FTIR analysis, precipitation of a calcium phosphate phase occurred. Furthermore, EDX analysis of the samples after incubation in SBF clearly indicated that precipitates were rich in calcium (Ca) and phosphorus (P). Also, incorporation of sodium (Na) and chlorine (Cl) into hydrogels from SBF was observed.

Fig. 7 shows concentrations of Ca and P measured in PBS and SBF during incubation of the hydrogels. On the one hand, the changes in concentration of Ca in media were related to release of the ions from BG particles. On the other hand, incorporation of calcium ions into hydrogels from biologically related fluids occurred at the same time. Simultaneously, an almost total reduction in P concentration just after 7-day incubation in SBF and gradual decrease during incubation in PBS was observed, confirming the intensive mineralization of all hydrogels containing BG particles.

As the A2 BG is a sufficiently rich source of Ca^{2+} ions for inducing supersaturation of PBS, the mineralisation process of the WPI/BG hydrogels occurred also in this medium. CaP precipitation on the surface of PCL-based composites containing A2 BG incubated in PBS was also observed in our previous work [13]. Incorporation of a bioactive ceramic phase in hydrogels, especially BGs, is one effective strategy for *in situ* mineralisation of hydrogels [14,31]. This approach can result in improvement of mechanical properties of hydrogels after implantation and also impart the ability to bond to bone, actively supporting the regeneration of bone tissue.

3.5. Enzymatic degradation

Incubation in both enzyme solutions resulted in increased mass loss of all materials with increasing incubation time, indicating ongoing degradation processes (Fig. 8). The presence of BG particles decreased degradation in both enzyme solutions, however reduction was visible after longer degradation periods (3 and 7 days). It seems that BG particle size and concentration did not influence the degradation process of composite hydrogels. Furthermore, the degradation was higher in trypsin. After 1-day incuba-

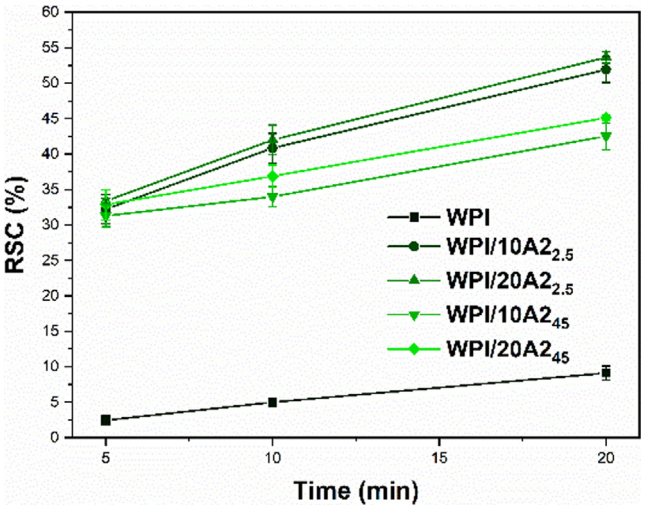

Fig. 9. Radical scavenging capacity (RSC) of WPI and WPI/BG hydrogels against the $ABTS^{\bullet+}$ radical as a function of time.

tion differences between materials incubated in trypsin and subtilisin were the most significant; mass loss for all materials was in the range 20 – 24 % and 10 – 16%, respectively. Furthermore, it was observed that mass loss after 7-day incubation in trypsin and subtilisin for pure WPI was 43% and 37%, respectively, while for composite hydrogels the values were in the range 27–30% and 22–27%, respectively.

Reduced enzymatic degradation of WPI/BG hydrogels compared to pure WPI material may be due to significantly lower open porosity of the composites (Fig. 1**B**), resulting in lower contact area of material surfaces with the enzyme solutions. Differences in degradation between WPI and WPI/BG hydrogels were observed only after longer incubation periods. This can indicate that, initially, enzyme action involved the exterior of materials. After longer incubation periods, degradation processes took place also in the interior, where porosity would be an important factor. Furthermore, the different cross-linking densities and bond strengths between the crosslinked protein chains, resulting from the presence of calcium ions in WPI/BG hydrogels' structure, may also alter enzymatic degradation [35].

Enzymatic degradation of protein-based biomaterials is one of the most important issues. This is due to the presence of many proteolytic enzymes during tissue healing and remodelling processes. Therefore, studying enzymatic degradation processes and understanding the factors affecting them is of crucial importance in designing biomaterials with controlled degradation rates for tissue engineering [36].

3.6. Radical scavenging capacity

The hydrogels' radical scavenging capacity against the $ABTS^{\bullet+}$ radical is shown in Fig. 9. WPI hydrogels showed relatively low

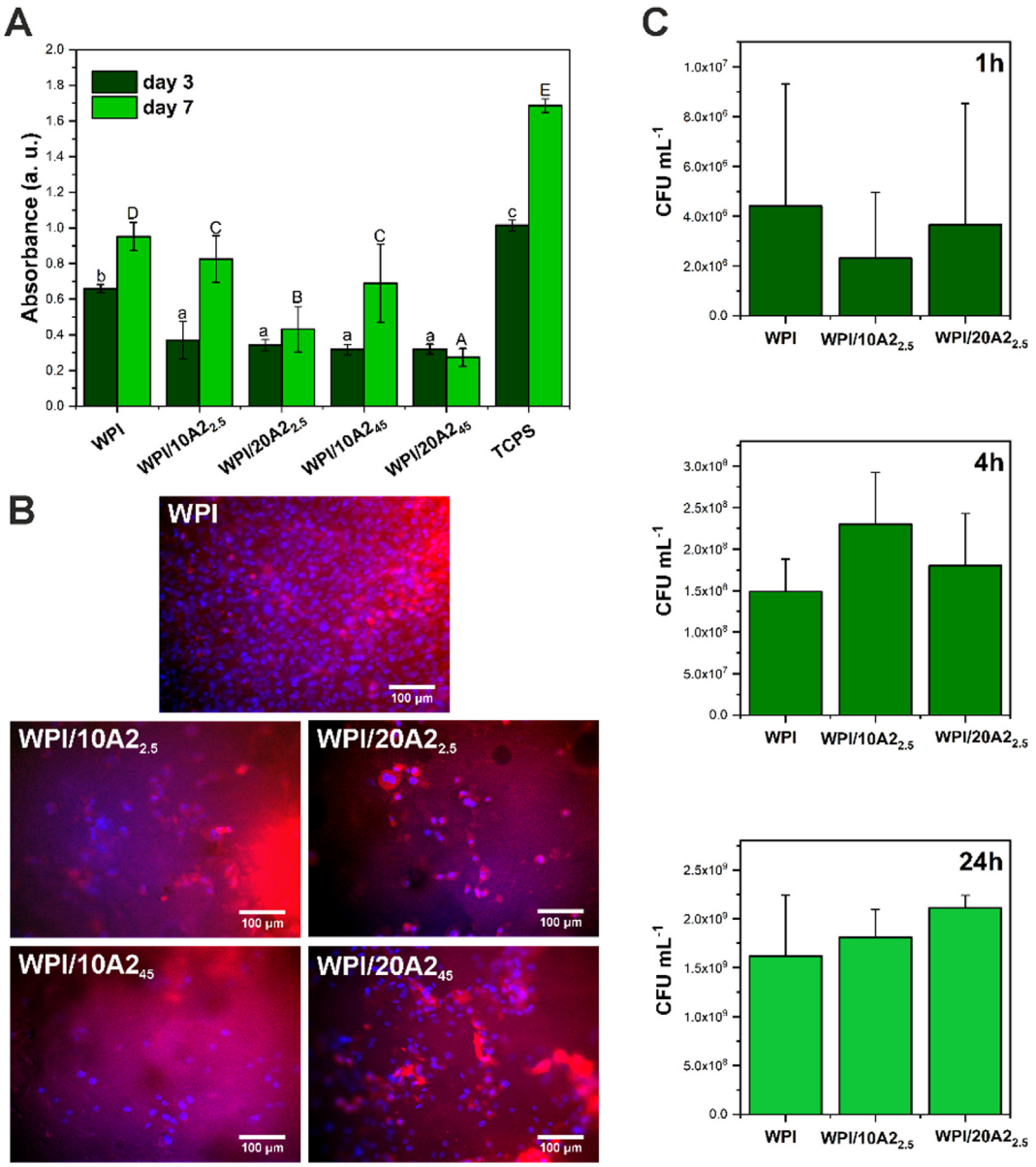

Fig. 10. Cell proliferation after 3- and 7-day culture of MG-63 cells on WPI and WPI/BG hydrogels (A). Statistically significant differences ($p < 0.05$) between materials are indicated by subsequent lower (for 3-day cell culture) and upper (for 7-day cell culture) Latin letters. Fluorescent microscopy images of MG-63 cells cultured for 7 days in direct contact with WPI and WPI/BG hydrogels (B). Red colour - cell membrane and cytoplasm; blue colour – cell nuclei. The results of CFU assay after 1, 4, and 24 h contact of *S. aureus* bacteria with WPI and WPI/BG hydrogels (C). Statistical analysis showed no differences ($p < 0.05$) between materials. (For interpretation of the references to colour in this figure legend, the reader is referred to the web version of this article.)

RSC, below 10% even after 20 min of contact with radicals, in contrast to the WPI/BG hydrogels. After 5 min, all of the composite hydrogels exhibited similar high RSC up to approximately 32%. The RSC of WPI/BG composites increased over time, reaching approximately 10% higher values for hydrogels with smaller BG particles (52–54%) compared to materials containing larger ones (43–45%). Interestingly, BG concentration did not affect the RSC significantly, however the values for hydrogels containing 20% of BG tended to be higher.

Radical scavenging capacity of whey proteins can be ascribed to the presence of amino acids residues that are prone to oxidation and therefore can scavenge radicals before they are able to damage other macromolecules. An example of such an amino acid is the cysteine residue in β-lactoglobulin with a free reactive thiol group (–SH). However, the antioxidant activity of these amino acids residues is greatly limited by the tertiary structure of the proteins, since they are not accessible to radicals [37]. One of the strategies for increasing antioxidant activity of proteins is disruption of their tertiary structure, i.e. protein denaturation. During heat treatment of WPI solution, protein unfolding (denaturation) and aggregation (gelation) occur. The obtained aggregates/gels showed high radical surface reactivity, ensured by accessible –SH groups. Furthermore, it has been shown that the presence of calcium ions in WPI solution markedly improved the level of protein denaturation and accessibility of radical scavenging thiol groups [38]. Therefore, the significantly higher radical scavenging capacity of WPI/BG hydrogels compared to WPI material may result from the aforementioned fast release of the Ca^{2+} ions from calcium-rich A2 BG. Smaller size of particles and their higher concentration may lead to faster release of Ca^{2+}, while also improving radical surface reactivity of hydrogels resulting from enhanced protein denaturation and higher accessibility of –SH groups. Radical scavenging capacity of WPI/BG composites did not arise from overall antioxidant activity of A2 BG particles, as was confirmed in our previous studies on poly(ε-caprolactone)/A2 composites [18,39].

The implantation of all biomaterials results in a foreign body response, involving generation of reactive oxygen species (ROS). Chronically high levels of ROS lead to oxidative stress which negatively affect tissue healing processes and may result in a number of pathological conditions [40]. Therefore, there is need to develop biomaterials with modulated antioxidant activity to support antioxidant mechanisms in human body.

3.7. In vitro biological tests

Fig. 10**A** presents the results of the MTS cell proliferation assay after 3 and 7 days of cell culture on the WPI-based hydrogels. It can be observed that addition of BG particles resulted in lower cell proliferation after day 3 in comparison to pure WPI. After 7 days, proliferation of cells seeded on the materials containing 10% of BG was noticeably higher in comparison to that on materials containing 20% of BG. There was no significant difference in cell proliferation after 3 or 7 days between WPI/10A2$_{2.5}$ and WPI/10A2$_{45}$ samples. The cell proliferation was the same on WPI/20A2$_{2.5}$ and WPI/10A2$_{45}$ samples on day 3 but was higher on WPI/20A2$_{2.5}$ than on WPI/10A2$_{45}$ on day 7. As expected, cell proliferation was the highest on control TCPS which is the optimized material for cell culture.

The aforementioned results were also confirmed by the microscopic observations (Fig. 10**B**). After 7 days of culture, the pure WPI sample was characterized by the highest number of cells from all the sample groups. Cells on WPI hydrogel reached confluency on day 7 in comparison to WPI/BG samples, where cells did not reach confluency even on day 7. However, the cells on all materials showed a flattened and well-spread morphology. It seems that after 7 days MG-63 cells were growing into the materials, as they seem to be covered by a thin layer of the hydrogel.

The results indicated that the higher the concentration of BG, the lower the cell proliferation. Those results might imply a positive influence of WPI/BG hydrogels on osteogenic cell differentiation, which needs to be further examined. Superb et al. [41] observed that increasing concentration of nano-sized BG in poly (3-hydroxybutyrate)-based composites induced reduction in MG-63 cell proliferation but enhanced alkaline phosphatase (ALP) activity and expression of an osteogenic marker – osteocalcin. In turn, Zamani et al. [42] showed no differences in proliferation of MG-63 cells on alginate/BG hydrogels, but they observed higher ALP activity on materials with higher concentrations of BG. The results confirmed our previous observations that WPI-based hydrogels are cytocompatible and support osteoblastic cell functions [7-9]. Therefore, they could be considered as biomaterials for bone tissue engineering applications.

3.8. Antibacterial activity

The results showed that WPI and WPI/BG hydrogels did not show any antibacterial effect against *S. aureus* after 1, 4, and 24 h contact time under the conditions tested (Fig. 10**C**). Furthermore, there were no statistically significant differences between samples without and with 10% and 20% of BG particles.

Antibacterial activity of highly soluble BG was previously reported in the literature [43]. The high concentrations of released calcium ions can change pH and osmotic pressure of the environment and can also alter bacterial membrane potential resulting in antibacterial properties of BG [44,45]. Our previous studies indicated that the presence of A2 BG particles in hydrogel matrices modulated their antibacterial action against *S. aureus* in a different manner – from full antibacterial activity of pectin/BG hydrogels [14] to a moderate antibacterial effect of GG/BG materials [31]. This can be related to different concentrations of BG particles in the polymer matrix; however the second possible explanation is the difference in hydrogel matrices and their interactions with BG particles, affecting e.g. Ca^{2+} ion release kinetics and amount.

4. Conclusions

In the present work, novel WPI-based hydrogels, modified with sol–gel-derived, calcium-rich BG particles were prepared and comprehensively evaluated. μCT analysis showed that hydrogels showed high porosity and nearly 100% interconnectivity of the pores. BG particles were generally homogenously distributed in the hydrogel matrix, affecting pore size, and reducing material porosity, depending on BG particle sizes and concentrations. Thermal analysis showed that the presence of BG particles in WPI matrices reduced water content in hydrogels and improved their thermal stability. Incorporation of inorganic particles led to a reduction of mechanical properties of the hydrogels. Swelling ratio of hydrogels depended on incubation medium and also size and concentration of BG particles. BG particles decreased enzymatic degradation of the materials. The results confirmed that the obtained composite hydrogels had the capacity to mineralize in simulated biological fluids (PBS and SBF) and possessed high radical scavenging capacity. Preliminary *in vitro* tests indicated that hydrogels were cytocompatible and supported MG-63 osteoblastic cell functions. The materials produced did not show any antibacterial effect against *S. aureus*. Importantly, the simple and inexpensive heat-induced gelation technique used allowed us to obtain ready-to-use, sterile materials, which is especially challenging in the case of hydrogels. The BG-containing WPI hydrogels displayed promising properties and are worthy of further *in vitro* and *in vivo*

investigation as inexpensive and widely available biomaterials for bone tissue regeneration.

Data availability

The authors declare that all the data related with this study are available within the paper or can be obtained from the authors on request.

CRediT authorship contribution statement

Michal Dziadek: Conceptualization, Methodology, Investigation, Formal analysis, Writing - original draft, Writing - review & editing, Visualization, Supervision, Project administration, Funding acquisition. **Katarzyna Charuza:** Investigation, Visualization, Writing - original draft. **Radmila Kudlackova:** Investigation, Visualization, Writing - original draft. **Jenny Aveyard:** Investigation, Visualization, Writing - original draft. **Raechelle D'Sa:** Investigation, Visualization, Writing - original draft, Funding acquisition. **Andrada Serafim:** Investigation, Visualization, Writing - original draft, Funding acquisition. **Izabela-Cristina Stancu:** Investigation, Visualization, Writing - original draft, Funding acquisition. **Horia Iovu:** Investigation, Visualization, Writing - original draft, Funding acquisition. **Jemma G. Kerns:** Investigation, Visualization, Writing - original draft. **Sarah Allinson:** Investigation, Visualization, Writing - original draft. **Kinga Dziadek:** Investigation, Visualization, Writing - original draft. **Piotr Szatkowski:** Investigation, Visualization, Writing - original draft. **Katarzyna Cholewa-Kowalska:** Resources, Writing - review & editing, Supervision, Funding acquisition. **Lucie Bacakova:** Writing - review & editing, Supervision. **Elzbieta Pamula:** Writing - review & editing, Supervision. **Timothy E. L. Douglas:** Conceptualization, Methodology, Writing - original draft, Writing - review & editing, Visualization, Supervision, Project administration, Funding acquisition.

Declaration of Competing Interest

The authors declare that they have no known competing financial interests or personal relationships that could have appeared to influence the work reported in this paper.

Acknowledgements

This work was supported by the N8 pump priming grant "Food2Bone" (TELD, RD'S) and National Science Centre, Poland, grant nos. 2017/27/B/ST8/00195 (KCK) and 2019/32/C/ST5/00386 (MD). The μCT investigations were possible due to European Regional Development Fund through Competitiveness Operational Program 2014-2020, Priority axis 1, ID P_36_611, MySMIS code 107066, INOVABIOMED (AS, ICS, HI). This work was partially financed by the Program "Excellent Initiative – Research University" for the AGH University of Science and Technology.

References

[1] S.H. Ralston, Bone structure and metabolism, Med. (United Kingdom) 41 (10) (2013) 581–585, https://doi.org/10.1016/j.mpmed.2013.07.007.
[2] R. Florencio-Silva, G.R.d.S. Sasso, E. Sasso-Cerri, M.J. Simões, P.S. Cerri, Biology of Bone Tissue: Structure, Function, and Factors That Influence Bone Cells, Biomed Res. Int. 2015 (2015) 1–17, https://doi.org/10.1155/2015/421746.
[3] S.J. Buwalda, K.W.M. Boere, P.J. Dijkstra, J. Feijen, T. Vermonden, W.E. Hennink, Hydrogels in a historical perspective: From simple networks to smart materials, J. Control. Release. 190 (2014) 254–273, https://doi.org/10.1016/j.jconrel.2014.03.052.
[4] H.B. Wijayanti, N. Bansal, H.C. Deeth, Stability of Whey Proteins during Thermal Processing: A Review, Compr. Rev. Food Sci. Food Saf. 13 (6) (2014) 1235–1251, https://doi.org/10.1111/crf3.2014.13.issue-610.1111/1541-4337.12105.
[5] M. Carson, J. Keppler, G. Brackman, D. Dawood, M. Vandrovcova, K. Fawzy El-Sayed, T. Coenye, K. Schwarz, S. Clarke, A. Skirtach, T.L. Douglas, Whey Protein Complexes with Green Tea Polyphenols: Antimicrobial, Osteoblast-Stimulatory, and Antioxidant Activities, Cells Tissues Organs. 206 (1-2) (2019) 106–118, https://doi.org/10.1159/000494732.
[6] T.E.L. Douglas, M. Vandrovcová, N. Kročilová, J.K. Keppler, J. Zárubová, A.G. Skirtach, L. Bačáková, Application of whey protein isolate in bone regeneration: Effects on growth and osteogenic differentiation of bone-forming cells, J. Dairy Sci. 101 (1) (2018) 28–36, https://doi.org/10.3168/jds.2017-13119.
[7] K. Norris, M. Kocot, A.M. Tryba, F. Chai, A. Talari, L. Ashton, B.V. Parakhonskiy, S. K. Samal, N. Blanchemain, E. Pamuła, T.E.L. Douglas, Marine-Inspired Enzymatic Mineralization of Dairy-Derived Whey Protein Isolate (WPI) Hydrogels for Bone Tissue Regeneration, Mar. Drugs. 18 (2020) 294, https://doi.org/10.3390/md18060294.
[8] M. Dziadek, R. Kudlackova, A. Zima, A. Slosarczyk, M. Ziabka, P. Jelen, S. Shkarina, A. Cecilia, M. Zuber, T. Baumbach, M.A. Surmeneva, R.A. Surmenev, L. Bacakova, K. Cholewa-Kowalska, T.E.L. Douglas, Novel multicomponent organic–inorganic WPI/gelatin/CaP hydrogel composites for bone tissue engineering, J. Biomed. Mater. Res. - Part A. 107 (11) (2019) 2479–2491, https://doi.org/10.1002/jbm.a.v107.1110.1002/jbm.a.36754.
[9] D. Gupta, M. Kocot, A.M. Tryba, A. Serafim, I.C. Stancu, Z. Jaegermann, E. Pamuła, G.C. Reilly, T.E.L. Douglas, Novel naturally derived whey protein isolate and aragonite biocomposite hydrogels have potential for bone regeneration, Mater. Des. 188 (2020) 108408, https://doi.org/10.1016/j.matdes.2019.108408.
[10] S.M. Rea, S.M. Best, W. Bonfield, Bioactivity of ceramic-polymer composites with varied composition and surface topography, J. Mater. Sci. Mater. Med. 15 (9) (2004) 997–1005, https://doi.org/10.1023/B:JMSM.0000042685.63383.86.
[11] Z. Neščáková, K. Zheng, L. Liverani, Q. Nawaz, D. Galusková, H. Kaňková, M. Michálek, D. Galusek, A.R. Boccaccini, Multifunctional zinc ion doped sol – gel derived mesoporous bioactive glass nanoparticles for biomedical applications, Bioact. Mater. 4 (2019) 312–321, https://doi.org/10.1016/j.bioactmat.2019.10.002.
[12] M. Mami, A. Lucas-Girot, H. Oudadesse, R. Dorbez-Sridi, F. Mezahi, E. Dietrich, Investigation of the surface reactivity of a sol-gel derived glass in the ternary system SiO 2 -CaO-P 2 O 5, Appl. Surf. Sci. 254 (22) (2008) 7386–7393, https://doi.org/10.1016/j.apsusc.2008.05.340.
[13] M. Dziadek, B. Zagrajczuk, E. Menaszek, K. Cholewa-Kowalska, A new insight into in vitro behaviour of poly(ε-caprolactone)/bioactive glass composites in biologically related fluids, J. Mater. Sci. 53 (6) (2018) 3939–3958, https://doi.org/10.1007/s10853-017-1839-2.
[14] T.E.L. Douglas, M. Dziadek, J. Schietse, M. Boone, H.A. Declercq, T. Coenye, V. Vanhoorne, C. Vervaet, L. Balcaen, M. Buchweitz, F. Vanhaecke, F. Van Assche, K. Cholewa-Kowalska, A.G. Skirtach, Pectin-bioactive glass self-gelling, injectable composites with high antibacterial activity, Carbohydr. Polym. 205 (2019) 427–436, https://doi.org/10.1016/j.carbpol.2018.10.061.
[15] T.E.L. Douglas, W. Piwowarczyk, E. Pamula, J. Liskova, D. Schaubroeck, S.C.G. Leeuwenburgh, G. Brackman, L. Balcaen, R. Detsch, H. Declercq, K. Cholewa-Kowalska, A. Dokupil, V.M.J.I. Cuijpers, F. Vanhaecke, R. Cornelissen, T. Coenye, A.R. Boccaccini, P. Dubruel, Injectable self-gelling composites for bone tissue engineering based on gellan gum hydrogel enriched with different bioglasses, Biomed. Mater. 9 (4) (2014) 045014, https://doi.org/10.1088/1748-6041/9/4/045014.
[16] B. Zagrajczuk, M. Dziadek, Z. Olejniczak, K. Cholewa-Kowalska, M. Laczka, Structural and chemical investigation of the gel-derived bioactive materials from the SiO2–CaO and SiO2-CaO-P2O5 systems, Ceram. Int. 43 (15) (2017) 12742–12754, https://doi.org/10.1016/j.ceramint.2017.06.160.
[17] T. Kokubo, H. Takadama, How useful is SBF in predicting in vivo bone bioactivity?, Biomaterials. 27 (15) (2006) 2907–2915, https://doi.org/10.1016/j.biomaterials.2006.01.017.
[18] M. Dziadek, K. Dziadek, K. Checinska, B. Zagrajczuk, M. Golda-Cepa, M. Brzychczy-Wloch, E. Menaszek, A. Kopec, K. Cholewa-Kowalska, PCL and PCL/bioactive glass biomaterials as carriers for biologically active polyphenolic compounds: Comprehensive physicochemical and biological evaluation, Bioact. Mater. 6 (6) (2021) 1811–1826, https://doi.org/10.1016/j.bioactmat.2020.11.025.
[19] J.A. Killion, S. Kehoe, L.M. Geever, D.M. Devine, E. Sheehan, D. Boyd, C.L. Higginbotham, Hydrogel/bioactive glass composites for bone regeneration applications: Synthesis and characterisation, Mater. Sci. Eng. C. 33 (7) (2013) 4203–4212, https://doi.org/10.1016/j.msec.2013.06.013.
[20] V.M. Azevedo, M. V. Dias, S. V. Borges, A.L.R. Costa, E.K. Silva, É.A.A. Medeiros, N. de F.F. Soares, Development of whey protein isolate bio-nanocomposites: Effect of montmorillonite and citric acid on structural, thermal, morphological and mechanical properties, Food Hydrocoll. 48 (2015) 179–188. https://doi.org/10.1016/j.foodhyd.2015.02.014.
[21] Raissa Alvarenga Carvalho Gomide, Ana Carolina Salgado Oliveira, Lucas Baldo Luvizaro, Maria Irene Yoshida, Cassiano Rodrigues Oliveira, Soraia Vilela Borges, Biopolymeric films based on whey protein isolate/lignin microparticles for waste recovery, J. Food Process Eng. 44 (1) (2021), https://doi.org/10.1111/jfpe.v44.110.1111/jfpe.13596.
[22] Breno Rocha Barrioni, Ana Celeste Oliveira, Maria de Fátima Leite, Marivalda de Magalhães Pereira, Sol–gel-derived manganese-releasing bioactive glass as a therapeutic approach for bone tissue engineering, J. Mater. Sci. 52 (15) (2017) 8904–8927, https://doi.org/10.1007/s10853-017-0944-6.
[23] Yanxia Li, Yanfeng Jiang, Fei Liu, Fazheng Ren, Guanghua Zhao, Xiaojing Leng, Fabrication and characterization of TiO2/whey protein isolate nanocomposite

film, Food Hydrocoll. 25 (5) (2011) 1098–1104, https://doi.org/10.1016/j.foodhyd.2010.10.006.
[24] A. Cagri, Z. Ustunol, E.T. Ryser, Antimicrobial, mechanical, and moisture barrier properties of low pH whey protein-based edible films containing p-aminobenzoic or sorbic acids, J. Food Sci. 66 (6) (2001) 865–870, https://doi.org/10.1111/jfds.2001.66.issue-610.1111/j.1365-2621.2001.tb15188.x.
[25] Emmanuelle Riou, Palatasa Havea, Owen McCarthy, Philip Watkinson, Harjinder Singh, Behavior of protein in the presence of calcium during heating of whey protein concentrate solutions, J. Agric. Food Chem. 59 (24) (2011) 13156–13164, https://doi.org/10.1021/jf203610k.
[26] C.M.B.S. Pintado, M.A.S.S. Ferreira, I. Sousa, Properties of whey protein-based films containing organic acids and nisin to control listeria monocytogenes, J. Food Prot. 72 (2009) 1891–1896, https://doi.org/10.4315/0362-028X-72.9.1891.
[27] Suraj Sharma, Igor Luzinov, Water Aided Fabrication of Whey and Albumin Plastics, J. Polym. Environ. 20 (3) (2012) 681–689, https://doi.org/10.1007/s10924-012-0504-8.
[28] Dattatreya M. Kadam, Mahendra Thunga, Sheng Wang, Michael R. Kessler, David Grewell, Buddhi Lamsal, Chenxu Yu, Preparation and characterization of whey protein isolate films reinforced with porous silica coated titania nanoparticles, J. Food Eng. 117 (1) (2013) 133–140, https://doi.org/10.1016/j.jfoodeng.2013.01.046.
[29] M. Betz, J. Hörmansperger, T. Fuchs, U. Kulozik, Swelling behaviour, charge and mesh size of thermal protein hydrogels as influenced by pH during gelation, Soft Matter. 8 (2012) 2477–2485, https://doi.org/10.1039/c2sm06976h.
[30] Wei Li, Yaping Ding, Shanshan Yu, Qingqing Yao, Aldo R. Boccaccini, Multifunctional Chitosan-45S5 Bioactive Glass-Poly(3-hydroxybutyrate- *co* -3-hydroxyvalerate) Microsphere Composite Membranes for Guided Tissue/Bone Regeneration, ACS Appl. Mater. Interfaces. 7 (37) (2015) 20845–20854, https://doi.org/10.1021/acsami.5b06128.
[31] Timothy E.L. Douglas, Michal Dziadek, Svetlana Gorodzha, Jana Lišková, Gilles Brackman, Valérie Vanhoorne, Chris Vervaet, Lieve Balcaen, Maria del Rosario Florez Garcia, Aldo R. Boccaccini, Venera Weinhardt, Tilo Baumbach, Frank Vanhaecke, Tom Coenye, Lucie Bačáková, Maria A. Surmeneva, Roman A. Surmenev, Katarzyna Cholewa-Kowalska, Andre G. Skirtach, Novel injectable gellan gum hydrogel composites incorporating Zn- and Sr-enriched bioactive glass microparticles: High-resolution X-ray microcomputed tomography, antibacterial and in vitro testing, J. Tissue Eng. Regen. Med. 12 (6) (2018) 1313–1326, https://doi.org/10.1002/term.v12.610.1002/term.2654.
[32] G. Gbassi, F. Yolou, S. Sarr, P. Atheba, C. Amin, M. Ake, Whey proteins analysis in aqueous medium and in artificial gastric and intestinal fluids, Int. J. Biol. Chem. Sci. 6 (2012) 1828–1837, https://doi.org/10.4314/ijbcs.v6i4.38.
[33] Yashar Rezaei, Fathollah Moztarzadeh, Sima Shahabi, Mohammadreza Tahriri, Synthesis, characterization, and in vitro bioactivity of sol-gel-derived SiO2-CaO-P2O5-MgO-SrO bioactive glass, Synth. React. Inorganic, Met. Nano-Metal Chem. 44 (5) (2014) 692–701, https://doi.org/10.1080/15533174.2013.783869.
[34] Wei Li, Patcharakamon Nooeaid, Judith A. Roether, Dirk W. Schubert, Aldo R. Boccaccini, Preparation and characterization of vancomycin releasing PHBV coated 45S5 Bioglass®-based glass-ceramic scaffolds for bone tissue engineering, J. Eur. Ceram. Soc. 34 (2) (2014) 505–514, https://doi.org/10.1016/j.jeurceramsoc.2013.08.032.
[35] Yulia Shmidov, Yumeng Zhu, John B. Matson, Ronit Bitton, Effect of Crosslinker Topology on Enzymatic Degradation of Hydrogels, Biomacromolecules. 21 (8) (2020) 3279–3286, https://doi.org/10.1021/acs.biomac.0c0072210.1021/acs.biomac.0c00722.s001.
[36] H. Azevedo, R. Reis, Understanding the Enzymatic Degradation of Biodegradable Polymers and Strategies to Control Their Degradation Rate, Biodegrad. Syst. Tissue Eng. Regen. Med. (2004), https://doi.org/10.1201/9780203491232.ch12.
[37] Alberto R. Corrochano, Vitaly Buckin, Phil M. Kelly, Linda Giblin, Invited review: Whey proteins as antioxidants and promoters of cellular antioxidant pathways, J. Dairy Sci. 101 (6) (2018) 4747–4761, https://doi.org/10.3168/jds.2017-13618.
[38] Aoife M Joyce, Alan L Kelly, James A O'Mahony, Controlling denaturation and aggregation of whey proteins during thermal processing by modifying temperature and calcium concentration, Int. J. Dairy Technol. 71 (2) (2018) 446–453, https://doi.org/10.1111/idt.2018.71.issue-210.1111/1471-0307.12507.
[39] M. Dziadek, K. Dziadek, B. Zagrajczuk, E. Menaszek, K. Cholewa-Kowalska, Poly (e-caprolactone)/bioactive glass composites enriched with polyphenols extracted from sage (Salvia officinalis L.), Mater. Lett. 183 (2016) 386–390, https://doi.org/10.1016/j.matlet.2016.07.077.
[40] David B. Gurevich, Kathryn E. French, John D. Collin, Stephen J. Cross, Paul Martin, Live imaging the foreign body response in zebrafish reveals how dampening inflammation reduces fibrosis, J. Cell Sci. 133 (5) (2020) jcs236075, https://doi.org/10.1242/jcs.236075.
[41] Superb K. Misra, Tahera Ansari, Dirk Mohn, Sabeel P. Valappil, Tobias J. Brunner, Wendelin J. Stark, Ipsita Roy, Jonathan C. Knowles, Paul D. Sibbons, Eugenia Valsami Jones, Aldo R. Boccaccini, Vehid Salih, Effect of nanoparticulate bioactive glass particles on bioactivity and cytocompatibility of poly(3-hydroxybutyrate) composites, J. R. Soc. Interface. 7 (44) (2010) 453–465, https://doi.org/10.1098/rsif.2009.0255.
[42] D. Zamani, F. Moztarzadeh, D. Bizari, Alginate-bioactive glass containing Zn and Mg composite scaffolds for bone tissue engineering, Int. J. Biol. Macromol. 137 (2019) 1256–1267, https://doi.org/10.1016/j.ijbiomac.2019.06.182.
[43] D. Zhang, O. Leppäranta, E. Munukka, H. Ylänen, M.K. Viljanen, E. Eerola, M. Hupa, L. Hupa, Antibacterial effects and dissolution behavior of six bioactive glasses, J. Biomed. Mater. Res. - Part A. 93 (2010) 475–483, https://doi.org/10.1002/jbm.a.32564.
[44] Z. Nazemi, M. Mehdikhani-Nahrkhalaji, M. Haghbin-Nazarpak, H. Staji, M.M. Kalani, Antibacterial activity evaluation of bioactive glass and biphasic calcium phosphate nanopowders mixtures, Appl. Phys. A Mater. Sci. Process. 122 (2016) 1063, https://doi.org/10.1007/s00339-016-0587-5.
[45] Eveliina Munukka, Outi Leppäranta, Mika Korkeamäki, Minna Vaahtio, Timo Peltola, Di Zhang, Leena Hupa, Heimo Ylänen, Jukka I. Salonen, Matti K. Viljanen, Erkki Eerola, Bactericidal effects of bioactive glasses on clinically important aerobic bacteria, J. Mater. Sci. Mater. Med. 19 (1) (2008) 27–32, https://doi.org/10.1007/s10856-007-3143-1.